X-Ray Fluorescence Correlation Spectroscopy: A Method for Studying Particle Dynamics in Condensed Matter

Jin Wang,[1] Ajay K. Sood,[1,*] Parlapalli V. Satyam,[1] Yiping Feng,[1] Xiao-zhong Wu,[2]
Zhonghou Cai,[1] Wenbing Yun,[1] and Sunil K. Sinha[1]
[1]*Experimental Facilities Division, Argonne National Laboratory, Argonne, Illinois 60439*
[2]*Department of Physics, Northern Illinois University, Dekalb, Illinois 60115*
and Materials Science Division, Argonne National Laboratory, Argonne, Illinois 60439
(Received 1 October 1997)

We have demonstrated that x-ray fluorescence correlation spectroscopy, in conjunction with microfocused synchrotron x-ray beams, can be used for elucidating particle dynamics. The dynamics of gold and ferromagnetic colloidal particles and aggregates undergoing both diffusion and sedimentation in water has been studied by measuring the time autocorrelation of the x-ray fluorescence intensity from a small illuminated volume. The dynamical parameters obtained are in excellent agreement with theoretical estimates and other measurements. Potential applications of the technique are discussed. [S0031-9007(97)05208-3]

PACS numbers: 83.10.Pp, 05.40.+j, 07.85.Qe, 78.70.En

Photon-correlation spectroscopy, probing fluctuations in scattered [1] or fluorescent [2,3] intensity to study particle dynamics in fluids, is well established in the visible light regime. With the advent of high-brilliance synchrotron radiation sources, correlation spectroscopy utilizing scattered radiation has only recently been extended to the x-ray wavelength regime by using spatially *coherent* x rays to study the time fluctuations of the corresponding speckle patterns [4–6]. Because x-ray fluorescence is an *incoherent* process, its intensity is simply proportional to the product of the number of fluorescent atoms in the x-ray beam and the x-ray exciting field intensity. Thus, x-ray fluorescence correlation spectroscopy (XFCS) does not require coherent x-ray beams. For an assembly of noninteracting particles undergoing diffusive motion, the fractional root-mean-square fluctuation in the number of particles in a given volume will be $\langle N\rangle^{-1/2}$, where $\langle N\rangle$ is the average number of particles in the given volume. If $\langle N\rangle$ is sufficiently small, such number fluctuations can be studied in real time, by measuring the time dependence of the fluorescence intensity $I_f(t)$ and its normalized autocorrelation function $g_f(t) = \langle I_f(0)I_f(t)\rangle/\langle I_f(0)\rangle^2$, thus yielding direct information about the particle dynamics. The small value of $\langle N\rangle$ can be realized with either a small illuminated sample volume, or a low particle concentration. This will necessitate a high x-ray beam intensity in order to get sufficient fluorescence signal from the small number of particles. With a Fresnel zone plate and third-generation synchrotron x-ray sources, such a high intensity microfocused x-ray beam is readily achievable [7]. A distinct advantage of the method is the element specificity by using an energy-dispersive x-ray detector. This method is particularly useful for studying both diffusive particle motion and flow in optically opaque systems for which methods employing visible light are not suited.

The fluorescence intensity from a collection of randomly moving particles with instantaneous positions $\mathbf{R}_i(t)$ is given by $I_f(t) = c\int d\mathbf{r} I_0(\mathbf{r})\sum_i \delta(\mathbf{r} - \mathbf{R}_i(t))$, where $I_0(\mathbf{r})$ is the spatial variation of the incident beam intensity and c is the fluorescent yield per particle. After taking Fourier transforms of $I_0(\mathbf{r})$, denoted by $\tilde{I}_0(\mathbf{k})$, and expressing the fact that positions of different particles are uncorrelated, the autocorrelation function yields $g_f(t) = 1 + (1/\langle N\rangle)[\int dk|\tilde{I}_0(\mathbf{k})|^2|f(\mathbf{k})|^2F(\mathbf{k},t)/|\tilde{I}_0(0)f(0)|^2]$, where N is the number of colloidal particles, and $F(\mathbf{k},t)$ is the single particle autocorrelation function given by $F(\mathbf{k},t) = \langle\exp\{i\mathbf{k}\cdot[\mathbf{R}_i(0) - \mathbf{R}_i(t)]\}\rangle$ and a form factor $f(\mathbf{k})$ for the particles has also been introduced to account for their finite sizes and shapes. The noninteracting limit is generally applicable to many of the systems that the method is best suited for. For example, given a detectable autocorrelation function intercept of 10^{-3} (or $\langle N\rangle = 10^3$, the upper limit of the number of particles in the illuminated volume), we estimate that the volume fraction of the particles is below 0.03 for particles with diameter less than 500 nm. For diffusive motion, $F(\mathbf{k},t) = \exp(-k^2D_t t)$, with D_t being the translational diffusion constant. For a uniform drift velocity $\mathbf{v}$, on the other hand, $F(\mathbf{k},t) = \exp(-i\mathbf{k}\cdot\mathbf{v}t)$. Finally, we take the form factor of $I_0(\mathbf{r})$ as $\exp[-(x^2 + y^2)/2\sigma^2]\exp(-z^2/2\sigma_z^2)$ with the beam propagating along the z direction. The beam size along the z direction, σ_z, as dictated by the sample thickness, is much larger than the beam size σ in the transverse (x-y) direction, and is taken to be essentially infinite for the purpose of the calculation. Therefore, the measurement is not sensitive to the diffusion in the z direction, and hence, probes particle motion only in the x and y directions. Carrying out the integrals explicitly, and setting the form factor $f(\mathbf{k}) \approx \exp(-R_g^2k^2/3)$ with R_g being the radius of gyration [8], we arrive at the result [3]

$$g_f(t) = 1 + \langle N\rangle^{-1}(1 + t/\tau_d)^{-1} \times \exp\{-t^2/[\tau_s^2(1 + t/\tau_d)]\}, \qquad (1)$$

 0031-9007/98/80(5)/1110(4)$15.00

where τ_d and τ_s are the translational diffusion and sedimentation time constants, respectively, $\tau_d = \sigma_{\text{eff}}^2/D_t$, $\tau_s = 2\sigma_{\text{eff}}/v$, $\sigma_{\text{eff}} = \sqrt{\sigma^2 + R_g^2/3}$, translational diffusion constant $D_t = k_B T/6\pi\eta R$, sedimentation velocity $v = 2\Delta\rho g R^2/9\eta$. Here, R is the hydrodynamic radius of the particle, η the viscosity of the solvent, k_B the Boltzmann constant, T the temperature, $\Delta\rho$ the density difference between the colloidal particles and water, and g the gravity acceleration. From Eq. (1), $\langle N\rangle = [g_f(0) - 1]^{-1}$, and therefore, fluorescence correlation spectroscopy has been used in the visible spectral region to estimate the particle concentration [9].

To demonstrate the usefulness of this method for elucidating particle dynamics, two types of samples were studied. First, colloidal gold particles, which have been studied by x-ray coherent intensity correlation spectroscopy [4], represented a good choice for the initial studies. Three colloidal gold samples of different particle sizes (denoted as samples 1 to 3) were studied to establish the relationship between particle dynamics and the particle size. Specifically, samples 1 and 2 were prepared using standard techniques [10] which yielded reasonably monodisperse colloidal particles of radii of approximately 100 and 200 nm, respectively, as determined by atomic force microscopy (AFM) performed on the gold colloids deposited on silicon substrates. Sample 3 was prepared by adding pyridine to the gold colloid suspension to reduce the stabilizing surface charge on the colloidal particles [11] resulting in colloidal aggregates of radii less than 900 nm, as measured by dynamic light scattering (DLS) and x-ray small angle scattering (XSAS). The dilute suspensions of gold particles had volume fractions ranging from 2×10^{-7} to 4×10^{-6}. The second type of sample, namely, a suspension of superparamagnetic microspheres (commonly referred to as ferrofluids, denoted as sample 4) was utilized to show the effect of the x-ray beam size to the measurements. This sample, with particle diameter 0.82 μm, as specified by the manufacturer (Bangs Laboratories, Inc., Fisher, IN), was diluted from 0.1 (as purchased) to 0.01 volume fraction with low conductivity deionized water.

The samples were measured during two separate synchrotron runs on the 2-ID undulator beam line at the Advanced Photon Source. For the gold particle samples, the colloidal suspensions were loaded in a thin walled quartz capillary tube of diameter 0.6 mm and placed in the focal spot of a microfocused beam of 12.4 keV photons, as illustrated schematically in Fig. 1. The focusing zone plate has a focal length of 76.5 mm with an estimated total beam intensity of approximately 2×10^8 photons/s at the focal point. The effective dimension of the illuminated volume was estimated to be approximately 1.9×10^3 μm^3. The fluorescence intensity from the sample was monitored by an energy-dispersive solid state detector placed as close as possible to the sample to maximize the solid angle acceptance. Discriminated by a single-channel analyzer, the gold $L\alpha$ fluorescence signal at about 9.7 keV was fed to a correlator (ALV 5000) that displays both the fluorescence intensity, $I_f(t)$, in real time and its normalized autocorrelation function, $g_f(t)$. The autocorrelation functions being presented were obtained by averaging over 5 to 10 runs, each of 120 s duration. The measurements on the ferrofluids were carried out with a similar experiment setup. Iron $K\alpha$ fluorescence lines at 6.4 keV were collected and the autocorrelation functions were measured with 1 to 2 runs, each of 600 s duration.

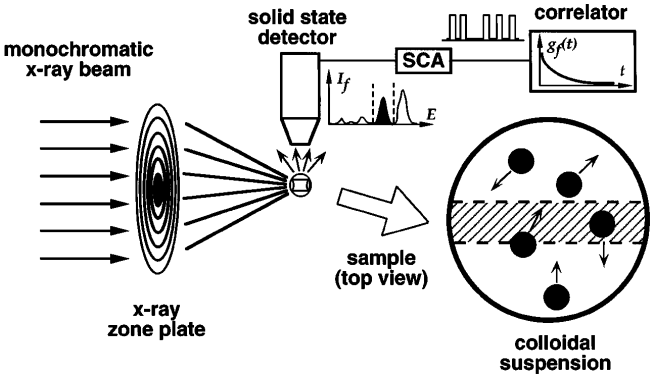

FIG. 1. Schematic of the experimental setup. The microfocused beam was obtained by first monochromating the beam from the undulator using a Si(111) double-crystal monochromator and then transmitting through a transmission Fresnel zone plate. A magnified view of sample is also sketched in the figure, where the shaded region outlines the x-ray illuminated area in the sample.

Shown in Fig. 2 are the averaged $g_f(t)$ measured for Fig. 2(A) sample 1, Fig. 2(B) sample 2, and Fig. 2(C) sample 3. The full theoretical expression given in Eq. (1) fits extremely well to the data. In the fitting procedure, the gold colloids are assumed to be monodisperse. Because of the divergent nature of the focused beam and the finite size of the capillary tube along the beam direction (z direction), an exact measure of the beam size in the x-y direction was not possible at the focal point. An estimate of the beam size was obtained as follows: For the initial fit to the correlation functions taken at the focal point, σ, R, and the intercept $g_f(0) - 1$ were all allowed to vary as fitting parameters. The average value (0.86 μm) of σ from different samples and different measurements was regarded as the measured beam size in the x-y direction. Subsequently, the correlation functions were fit with the remaining two parameters. The least-square-fitted values of the hydrodynamic radii of the particles are 102, 220, and 370 nm for samples 1, 2, and 3, respectively, in good agreement with the AFM, DLS, and XSAS measurements. The particle sizes for samples 1, 2, and 3 correspond to values of D_t of 2.1, 0.97, and 0.53 $\mu\text{m}^2/\text{s}$ and of v of 0.24, 1.1, and 3.2 $\mu\text{m}/\text{s}$, respectively. The corresponding time constants are listed in the figure. It can be seen that when $\tau_d \ll \tau_s$ (i.e., $\sigma_{\text{eff}} R^3 \ll 0.1$ μm^4 for gold colloids in water), the decay of $g_f(t)$ is governed by the diffusion process, i.e., $[g_f(t) - 1] \propto 1/(1 + t/\tau_d)$ with $\tau_d \propto R\sigma^2$. In the

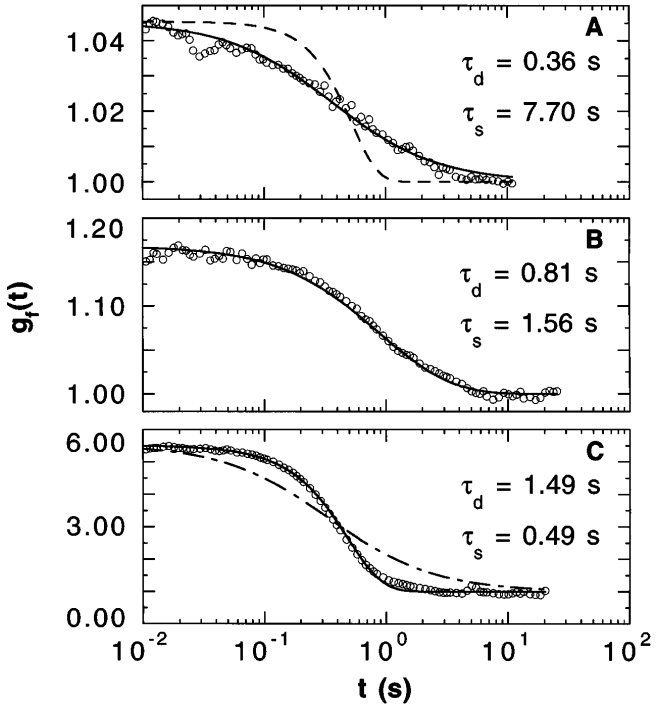

FIG. 2. The experimental (circles) and theoretical (line) fluorescence autocorrelation functions for samples 1 (A), 2 (B), and 3 (C). The diffusion and sedimentation time constants (τ_d and τ_s, see text for the definitions) are also shown in the figure. Two theoretical simulations are also presented using only the sedimentation model [dashed line in (A)] or only the diffusion model [dash-dotted line in (C)].

opposite limit ($\tau_d \gg \tau_s$), $[g_f(t) - 1] \propto \exp(-t^2/\tau_s^2)$ with $\tau_s \propto R^{-2}\sigma$. The time constants obtained from the fits indicate that the diffusion of particles is the dominant dynamic process, observed by the XFCS measurement under the given experimental conditions, in samples 1 and 2. When the particle size is larger, as in sample 3, the decay of the fluorescence autocorrelation function is mainly governed by the sedimentation time τ_s. Therefore, in this case, the XFCS measurement is more sensitive to the sedimentation than the diffusion of the particles. It should be noted that the translational diffusion and sedimentation processes have very distinct forms for the correlation function. The translational diffusion dominated correlation function decays approximately as t^{-1} and the sedimentation governed correlation function decays as $\exp(-t^2/\tau_s^2)$. To illustrate this, fits to the correlation functions using only the sedimentation model [dashed line in Fig. 2(A)] or the diffusion model [dash-dotted line in Fig. 2(C)] are also included.

To demonstrate the effect of x-ray beam size on XFCS measurements, we also studied the ferrofluids (sample 4) at different locations along the zone plate axis and corresponding to different distances d from the focal point. Away from the focal point, the beam size σ is directly proportional to d. Although iron is a relatively light atom, its x-ray fluorescence signal from the sample was sufficiently intense to penetrate through the solution and to be picked up by the detection system with adequate counting statistics. The correlation functions of iron fluorescence at and 12 mm away from the focal point are shown in Fig. 3(A) with theoretical fits according to Eq. (1). In the fitting procedure, τ_d, τ_s, and the intercept $\langle N \rangle^{-1}$ were all allowed to change as the fitting parameters. The theoretical fit to the correlation function reveals that the correlation function measured at the focal point is more sensitive to the diffusive motion of microspheres. On the other hand, the correlation functions measured far away from the focal point are more sensitive to the sedimentation. This is demonstrated more clearly in Fig. 3(B) where the fitting parameters τ_d and τ_s are plotted as a function of d. With excellent agreement with the theoretical predictions, τ_d is proportional to d^2 while τ_s is proportional to d when d is beyond about 4 mm (fits not shown). As d increases to about 5 mm, where $\tau_d > \tau_s$, the beam size becomes so large that the parameters related to diffusion may not be accurately measured. This indicates the necessity of using microsized x-ray beams in the measurement. The reliability of the fitting parameters is further verified by the fact that hydrodynamic radius R of the microspheres, derived from $R \propto \tau_d^{-2/5}\tau_s^{1/5}$ at each position [dots in Fig. 3(B)], is approximately constant, with a mean value of 0.71 μm [dashed line in Fig. 3(B)]. The measured R value was

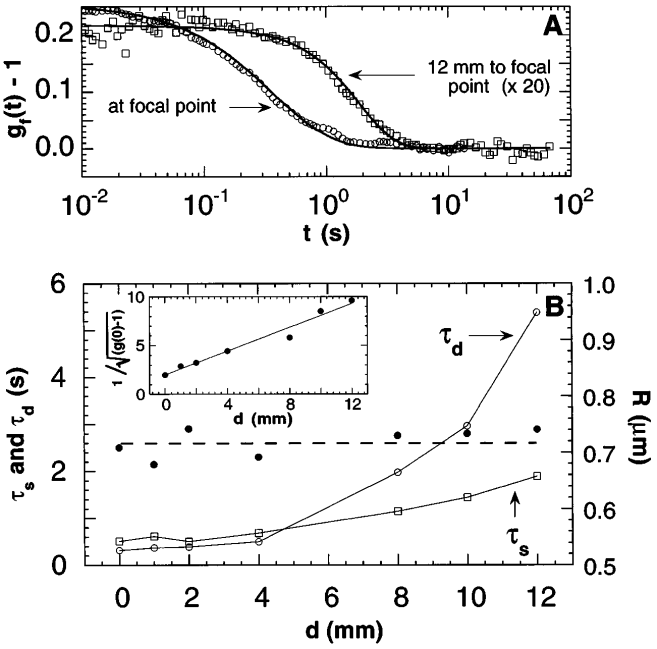

FIG. 3. Experimental results for sample 4 measured at different positions, on the zone plate axis, at a distance d to the focal point. (A) The experimental (circles and rectangles) and theoretical (line) fluorescence autocorrelation functions at and 12 mm away from the focal point. (B) The fitting parameters τ_d (circles), τ_s (rectangles), and derived values of R (dots) at each position are shown. The solid lines connecting data points are for guiding the eye. The dashed line represents the mean value of R. The inset for (B) shows the relationship between $[g_f(0) - 1]^{-1/2}$ and d (dots) and the linear function fit (solid line).

almost twice as large as the value specified by the manufacturer. It was not possible to characterize the same system with our DLS experimental setup because at this concentration (0.01 volume fraction) the sample is opaque. Transmission electron microscopy (TEM) studies of deposited and evaporated film of the suspension did reveal the existence of a large number of larger particles with a significant degree of polydispersity, implying that the present fits, while agreeing well with the data, should be taken as yielding only average parameters for particle sizes. As shown in Eq. (1), the intercept of the correlation function should be proportional to $\langle N \rangle^{-1}$. Thus, $[g_f(0) - 1]^{-1/2}$, a value directly derived from one of the fitting parameters, $g_f(0)$ should be proportional to the beam size σ or, in turn, to d. This has been clearly observed in the experiment [shown as the inset for Fig. 3(B)]. It is worth mentioning here that $g_f(0)$ can be regarded as a model-independent fitting parameter and that the value of $g_f(0)$ is highly reliable.

We have demonstrated a new and powerful technique to probe the dynamics of colloidal particles by real-time analysis of x-ray fluorescence intensity fluctuations. While the model for independent particles diffusion and sedimentation fits our data well for the present dilute colloidal systems, it would be obviously of interest to study deviations from the model as the concentration of particles is increased to show interaction effects. We estimate that samples with particle concentration up to 10 times higher than those being examined could still be studied with the technique, which will be the subject of future studies. Furthermore, with the attainment of the maximum achievable intensities in microfocused beams at current synchrotron sources and optimization of the solid angle subtended by the detector, the limits of the technique could be extendible to particles containing 10^5 fluorescent atoms. The element specificity and the high sensitivity of the x-ray fluorescence makes XFCS a particularly unique probe. Parenthetically, we also note that the concept of XFCS was independently proposed by Goulon *et al.* [12]. However, without the microfocused x-ray beams, such an idea had never been realized. Furthermore, coherent x rays, which are required for other x-ray photon correlation spectroscopy techniques, are not needed for this method. There have been one or two examples of the use of noncoherent x-ray beams to study slow dynamics of large particles. Wakabayashi [13] used the time-autocorrelation functions of the Bragg reflected intensity to study the rotational diffusion of the particles. One may also use a host of alternative x-ray focusing devices [14] for achieving a microfocused x-ray beam.

We conclude with a listing of some of the novel possibilities opened up for study with this technique. These include the study of the motion of biological macromolecules containing heavy atoms on or across membranes; the study of interdiffusion of atoms at interfaces between two species of materials; the study of the sedimentation or flow of colloidal particles in fluids containing polymers or surfactants which, we note, is unobservable by coherent x-ray intensity correlation spectroscopy techniques; the study of glass transitions or phase separations in liquid using tracer particles of gold or other colloids to probe the dynamics, and the study of the diffusion of particles through gels and other porous media. An interesting variant would be the study of magnetic domain dynamics or domain wall motion using circularly polarized beams and the magnetic circular dichroism effect.

We thank H. Zhao and A. Wong for their assistance and the entire 2-ID beam line staff at the Advanced Photon Source for their technical support. We also thank R. E. Cook for the TEM measurements. This work is supported by the U.S. Department of Energy, BES-Materials Science, under Contract No. W-31-109-ENG-38, and is partially supported by the State of Illinois under HECA.

*On leave from Department of Physics, Indian Institute of Science, Bangalore 560012, India.

[1] B. Chu, *Laser Light Scattering: Basic Principles and Practice* (Academic Press, Boston, 1991).
[2] D. Magde, E. Elson, and W. W. Webb, Phys. Rev. Lett. **29**, 705 (1972).
[3] B. J. Berne and R. Pecora, *Dynamic Light Scattering: with Applications to Chemistry Biology, and Physics* (John Wiley & Sons, New York, 1976).
[4] S. B. Dierker, R. Pindak, R. M. Fleming, I. K. Robinson, and L. Berman, Phys. Rev. Lett. **75**, 449 (1995).
[5] S. Brauer, G. B. Stephenson, M. Sutton, R. Brüning, E. Dufresne, S. G. J. Mochrie, G. Grübel, J. Als-Nielsen, and D. L. Abernathy, Phys. Rev. Lett. **74**, 2010 (1995).
[6] S. G. J. Mochrie, A. M. Mayes, A. R. Sandy, M. Sutton, S. Brauer, G. B. Stephenson, D. L. Abernathy, and G. Grübel, Phys. Rev. Lett. **78**, 1275 (1997).
[7] A. A. Krasnoperova, J. Xiao, F. Cerrina, E. Di Fabrizio, L. Luciani, M. Figliomeni, M. Gentili, W. Yun, B. Lai, and E. Gluskin, J. Vac. Sci. Technol. B **11**, 2588 (1993).
[8] O. Glatter and O. Kratky, *Small Angle X-Ray Scattering* (Academic Press Inc., New York, 1982).
[9] Z. Huang and N. L. Thomson, Biophys. J. **70**, 2001 (1996).
[10] G. Frens, Nature (London) **241**, 19 (1973).
[11] P. Dimon, S. K. Sinha, D. A. Weitz, C. R. Safinya, G. S. Smith, W. A. Varady, and H. M. Linsay, Phys. Rev. Lett. **57**, 595 (1986).
[12] J. Goulon, C. Goulon, C. Gauthier, and H. Emerich, in *Particle and Fields Series 49: Synchrotron Radiation and Dynamic Phenomena*, edited by A. Beswick (American Institute of Physics, New York, 1991), pp. 420–427.
[13] N. Wakabayashi (unpublished).
[14] E. A. Stern, Z. Kalman, A. Lewis, and K. Lieberman, Appl. Opt. **27**, 5135 (1988); D. H. Bilderback, S. A. Hoffman, and D. J. Thiel, Science **263**, 201 (1994); A. Snigirev, V. Kohn, I. Snigireva, and B. Lengeler, Nature (London) **384**, 49 (1996); J. Wang, M. J. Bedzyk, and M. Caffrey, Science **258**, 775 (1992); Y. P. Feng, S. K. Sinha, H. W. Deckman, J. B. Hastings, and D. P. Siddons, Phys. Rev. Lett. **71**, 537 (1993).